

Simulation Study Of Multi-Layered Active Region Uv Photo-Detector For High Efficient Photoactive Semiconductors

A.Alfred Kirubaraj, S.Senith, Jerrin Issac Sam S, P.S.Athira, S.R.Jino Ramson

Abstract: UV photo-detective transducers converts light energy in the range of 40 nm to 400 nm into electrical output with high visible rejection ratio. Recently, a study is done to reduce the thickness of active layer with a high refractive index metal layer in between low refractive index oxide layer. In this paper, we present a novel method in designing a thin-layered TiO₂/Ag/TiO₂ (TAT structure) active region photo-detector with Pt metal electrodes. The designed 2D structure with TiO₂ and 3D structure with TAT as active layer are developed with semiconductor and Opto-electronics module. The developed design shows considerably high output current response of 0.077 A/W and 4.9 A/W with 5 V as applied bias for TiO₂ and TAT active region respectively. Also, the study on dark current is modelled through MATLAB. The simulation study shows, the variation in dark current response with respect to work function of metal electrode and thickness of TAT layer. The proposed TAT structure develops less leakage current of 4.6284 nA as compared to the conventional structure producing in micro ampere range. Hence the proposed designed structure with high output current response with less dark current can be applied in high sensitivity sensor, thin film solar cells, photo active semiconductors and in photonics.

Index Terms: Photo-detector, TiO₂, TAT, Pt electrodes.

I. INTRODUCTION

Photo-detectors are semiconductor devices that convert incident light into current by the generation of electron-hole pairs. The generated electron-hole pairs produce high output current response which can be used in various high efficient semiconductor applications. Recently, for the fabrication of ultraviolet light photo-detector, TiO₂ is associate correct material that has involved a lot of thought attributable to their acceptable properties within the ranges of close to infrared and visual. It a tall ratio yet nearly as good chemical and mechanical properties and has been the fabric of best for the fabrication of electrical conduction switches [1]-[3]. UV photo-detectors exhibits maximum output current response in the UV range (10 nm – 400 nm) and shows maximum visible and IR rejection ratio. The III-N photo-detectors prepared on PSS exhibits low dark current. Photo-detector with ZnO active region shows high output current response due to decrement of recombination rate. GaAs nanowire photo-detector device exhibits high output current response.

In comparison to III-N (GaN) and III-V (GaAs) detector shows suppression in dark current while silicon PD offers high sensitivity and operational speed [4-5]. With oxygen plasma treatment (fabrication process) the output response shows up to 153 A/W due to photo-chemical filling of trap states [6]. There is a drive to reduce the thickness of active region of photo-detector to enhance the efficiency. However, reducing the thickness of active layer thin film leads to the reduction in the amount of light absorbed. As a solution we are using light trapping mechanism. Silver particles are exposed to improve optical features of TiO₂ based photo-detectors. Optical properties of photo-detectors depend on optical properties of silver nanoparticles. Photo-detector with doped Ag nanoparticles of size 5 nm – 50nm shows high light trapping capability [7]. Photo-detectors with TiO₂ films deposited by RF magnetron Sputtering shows low dark current due to the achievement of high stoichiometric films [8-9]. Under white-light illumination, the responsivity was in excess of 1500 A/W which is higher than that of conventional photo-detectors with the semi-transparent polycrystalline silicon gate [10-11]. Silicon-on-insulator (SOI) provides distinctive characteristics to photo-detectors based on optical and carrier confinement, results in improved light absorption and detection of photo-generated carriers, respectively [12]. The organization of the report as follows: Chapter II talks about the introduction of UV TiO₂ based photo-detector and TAT based photo-detector with Au metal electrodes with conventional technique, chapter III talks about the proposed TAT based detector with Pt electrodes, chapter IV includes the simulation results and its discussions of 2D TiO₂ based photo-detector and 3D TAT based photo-detector and chapter V gives the conclusion of the proposed TAT UV photo-detector.

II. CONVENTION PHOTO-DETECTOR

A. TiO₂ based photo-detector

The current development of electrical conduction semiconductor applications needs ecologically stable, clear, and method consistent materials. Amongst, TiO₂ materials have several fascinating proper-ties within the ranges of near-IR and visual also in the fabrication of UV photo-detector. It can be widely utilized in optics, optoelectronics, sensors and medical specialty sciences.

Manuscript published on 30 March 2019.

*Correspondence Author(s)

A.Alfred Kirubaraj & Athira, ECE, Karunya Institute of Technology and Sciences, Coimbatore, India.

S.Senith & Jerrin Issac Sam, MBA, Karunya Institute of Technology and Sciences, Coimbatore, India.

Jino Ramson, Engineering Technology, Purdue University, USA.

© The Authors. Published by Blue Eyes Intelligence Engineering and Sciences Publication (BEIESP). This is an [open access](https://creativecommons.org/licenses/by-nc-nd/4.0/) article under the CC-BY-NC-ND license <http://creativecommons.org/licenses/by-nc-nd/4.0/>.

B. TAT based photo-detector with Au electrodes

There is a requirement to scale back the breadth of active layer in photo-detector to boost the efficiency of extracting the generated carriers. However, dropping the thickness of skinny film additionally reduces the amount of sunshine absorbed. To unravel this down-side we are able to use lightweight saddlery mechanism. Silver nanoparticles with precise diameters area unit exposed to extend optical features of TiO₂ primarily based photo-detectors. Figure one shows the TAT primarily based photo-detector with gold (Au) metal electrodes. Optical properties of photo-detectors be determined by the optical properties of nanoparticles. thus for the photo-detector application we want to recognize that of those properties area unit helpful then style appropriate nanoparticle to maximize these impact whereas minimizing unwanted optical properties. Nanoparticles diameter is often between 5-100 nm. If the diameter of nanoparticles is regarding quite one hundred nm, lightweight won't be absorbed with efficiency, and once it's smaller than 5 nm, charge transition through channels fades and scattering is accrued. The recent study shows, adding material impurities can affect the compound semiconductors. To over this effect, use of ultra-thin metal with high refractive dielectrics can be employed for good conducting oxides.

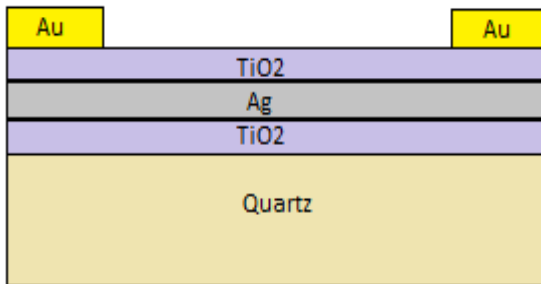


Fig. 1:TAT based photo-detector with Au metal electrodes

III. PROPOSED DESIGN NOVELTY

A. TAT based photo-detector with Pt electrodes

The noble metal (Pt) has been used as a stable Schottky contact to TiO₂ because of its high metal work perform (6.76 eV). RF-sputtered TiO₂ ultraviolet light PDs exploitation Au because the Schottky metal have larger dark current. Figure 2 shows the proposed TAT structure with (Pt) metal electrodes having the massive work-function metal platinum ($\Phi = 6.76$ eV). High work function is employed to increase the barrier height to reduce the dark current as the generated charge carriers needs more energy to cross the barrier.

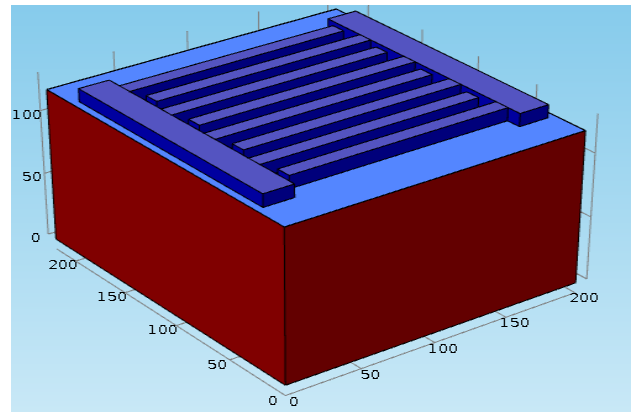


Fig. 2: TAT based photo-detector with Pt metal electrodes

IV. SIMULATION RESULTS AND ITS DISCUSSIONS

A. Simulation of TiO₂ and TAT based photo-detectors

Table 1: Variation of output current with wavelengths of TiO₂ UV photo-detector

Wavelength (nm)	Output current response (A)
90	0.024
120	0.012
220	0.0342
250	0.05
360	0.077
400	0.0325
710	0.038

Table 1 specifies the variation in output current response for different wavelengths of TiO₂ UV photo-detector. It shows that the UV photo-detector exhibits a maximum output current response of 0.077 A at 360 nm showing high visible rejection ratio.

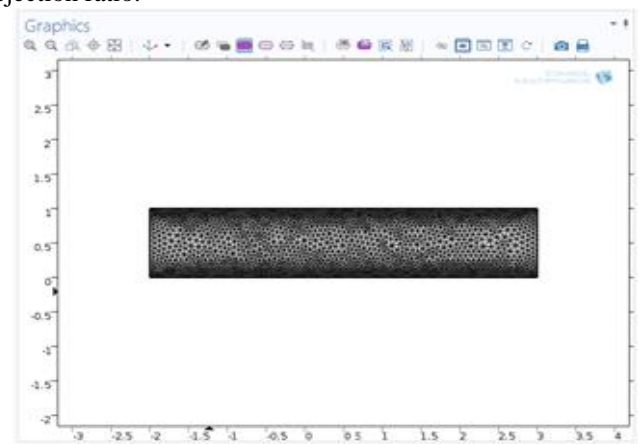


Fig. 3: Meshed view of 2D structure

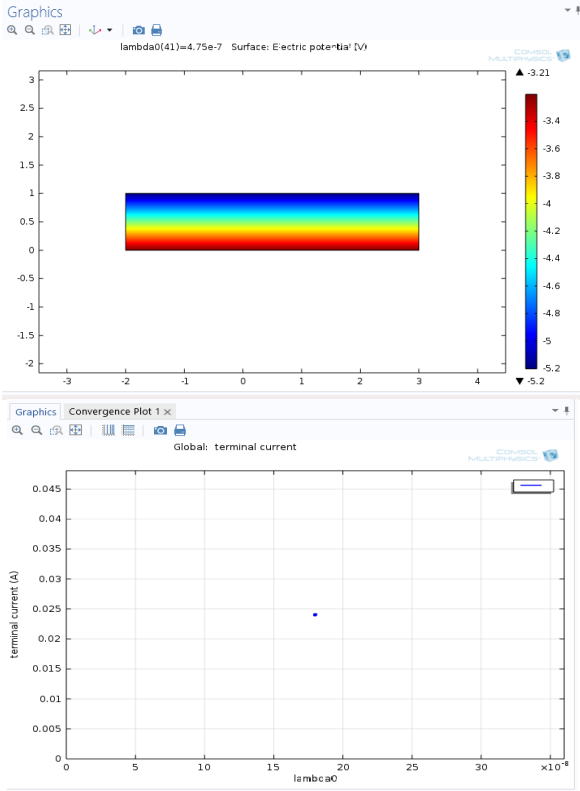


Fig. 4: Electric potential distribution of 2D structure
Fig. 5: Output current response at 90nm

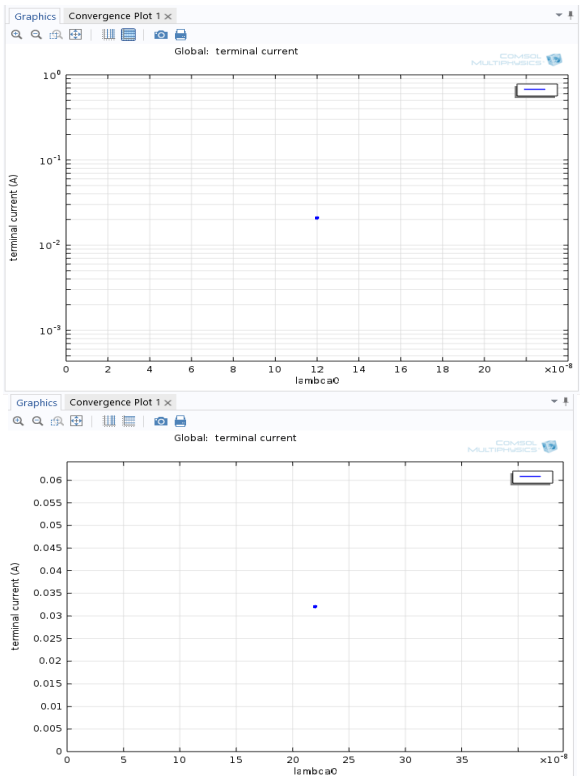


Fig. 6: Output current response at 120 nm
Fig. 7: Output current response at 220 nm

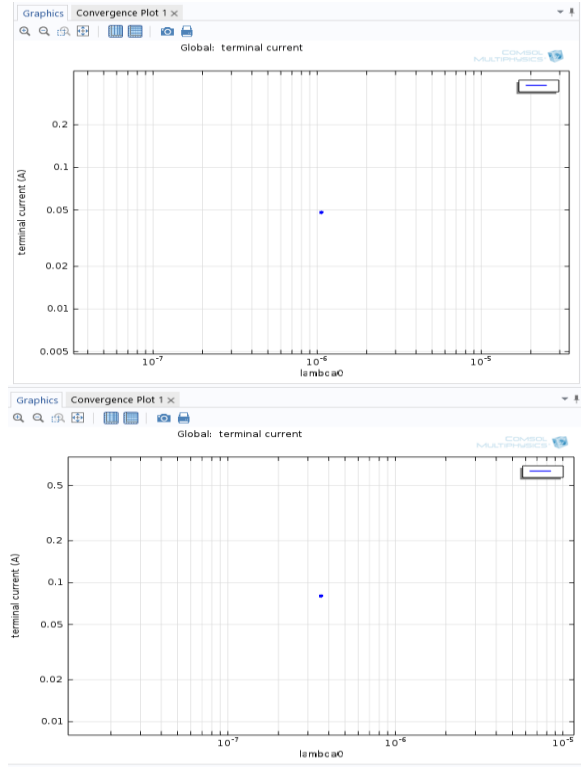


Fig. 8: Output current response at 250 nm
Fig. 9: Output current response at 360 nm

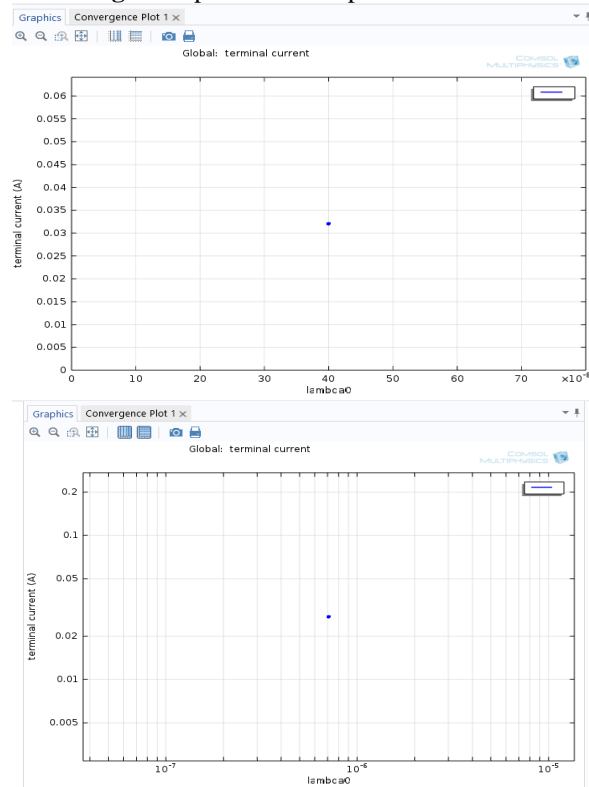


Fig. 10: Output current response at 400 nm
Fig. 11: Output current response at 710 nm

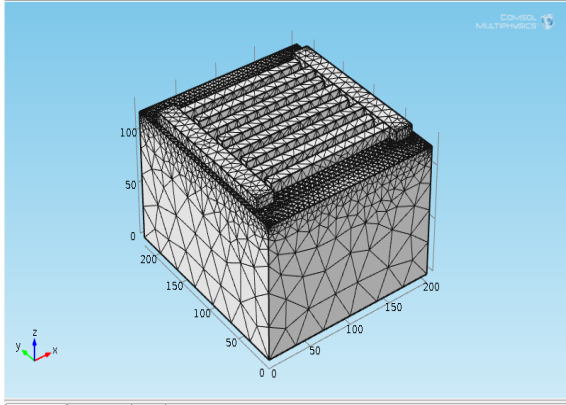
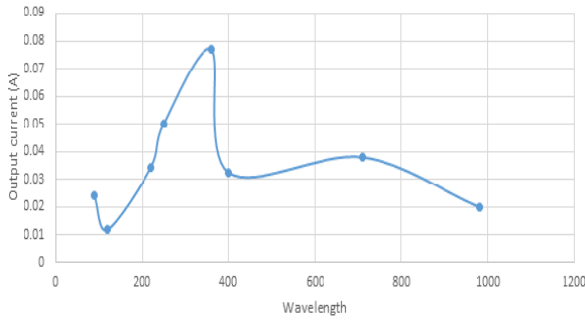


Fig. 12: Variation of TiO₂ output current response
 Fig. 13: Meshed view of 3D TAT photo-detector

distribution of the 2D structure which gives a maximum negative potential at the top of the structure where the biasing potentials are applied. Figure 5, 6, 7, 8, 9, 10, 11 shows the output current response of TiO₂ based photo-detector at 90 nm, 120 nm, 220 nm, 250 nm, 360 nm, 400 nm, 710 nm respectively. Plotting of graph between variations in output current response with wavelengths of TiO₂ UV photo-detector is shown in Figure 12. Figure 13 shows the meshed view of TAT based photo-detector and Figure 14 shows the electric potential distribution of the TAT based photo-detector and Figure 15 shows the plot of variation of output current response with wavelengths of TAT UV photo-detector. The analysis shows that, with the application of light trapping mechanism to conventional TiO₂ UV photo-detector, the absorption efficiency of active region is increased that results in huge rise in output current of 4.9 A at 360 nm. This light-weight saddlery mechanism will increase the carrier life time, carrier generation and conjointly reduces the recombination rate of electron-hole pairs which ends up in dark current reduction and thermal noise.

A. Dark current simulation using MATLAB

In applied dark current condition, the space charge in the active region has two flow process: First process due to Electron arrest into active region and Second process due to Thermo-emission of electrons from them. Among the two process, the dark current is prominent in thermos-emission process. Considering the simplified structure under no light exposure of a photo-detector with TAT multi-layered active region as {k = 1, 2,..., M} layers of active region, and each layer has <Nk> average number of electrons. The drift current in the active region raises due to electrons captured is governed by:

$$\langle J_d \rangle = \frac{q \sum QRG_K}{P_K} \tag{1}$$

From above equation, J_d is the dark current, density, (q) is the electron charge, G_k is the electron thermo-excitation and P_K is the probability of electron capture.

The condition satisfying (qV>qV0>>KT), the mobile carriers injected from the emitter contact reach the first QRs layer plane and then overcome the barrier height (qV0=EQR). Hence the equation 1 can be re-written as:

$$J_d = \frac{J_m \exp(q(\langle \phi \rangle + \phi))}{KT} \tag{2}$$

The resultant average current density is on integration over the in-plane coordinates as:

$$\langle J_d \rangle = \sum_{QR} \int_{-lqr}^{lqr} J_d dx dy \tag{3}$$

Solving above equation by numerical methods, we have the final equation for dark current will be:

$$\langle J_d \rangle = \frac{21.45}{\phi} \operatorname{erf}(0.48 * q * lqr * \sqrt{\frac{x^3}{\epsilon KT}} * \sqrt{\sum QR}) * \frac{\epsilon KT}{q^2} * \sqrt{\sum QR} * \frac{q(v + C_1 - C_2)}{(M + 1)KT}$$

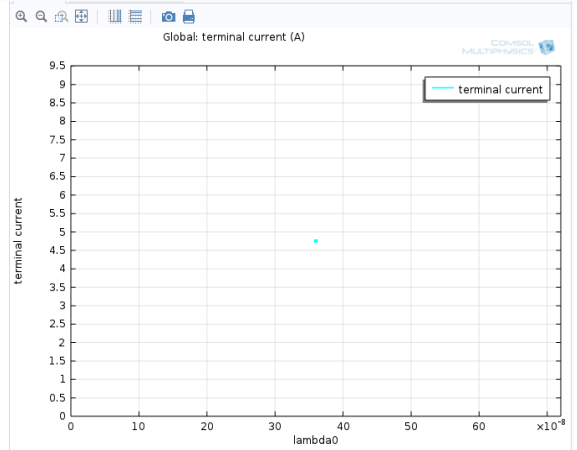
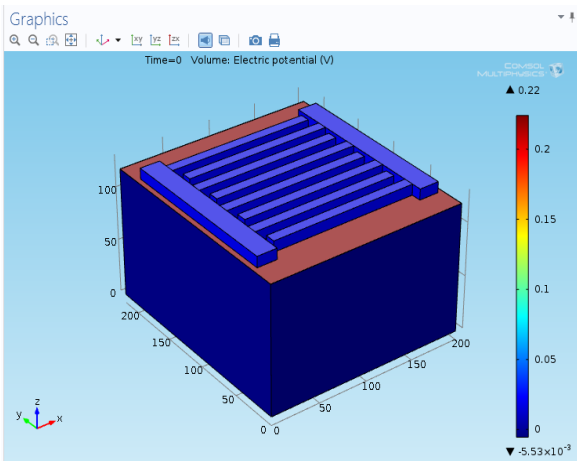


Fig. 14: Electric potential distribution of 2D structure
 Fig. 15: Output current response of TAT UV

Photo-detector at 360 nm

Figure 3 shows the meshed view of 2D TiO₂ based photo-detector which divides the structure into grids for the simulation and Figure 4 shows the electric potential



Where

$$C_1 = \frac{2 \Pi q}{\epsilon} (M(M+1)x \Sigma D) \quad \text{and}$$

$$C_2 = \frac{2 \Pi q}{\epsilon M * x * \sqrt{\Sigma QR}} (M(M+1)) \Sigma QR * x(1-0.32)$$

In which ΣQR , ΣD , x , ϕ stands for the number of active layers in active region, the donor density of active region, the transverse spacing between metal electrodes and the work function of metal electrodes.

Table 2: Variation of dark current with different work function metals.

Material	Work function (eV)	Dark current (A)
Gold (Au)	3.43	4.6284×10^{-9}
Nickel (Ni)	5.2	1.1139×10^{-9}
Platinum (Pt)	6.76	9.0724×10^{-10}

Table 2 specifies the variation in dark current response for different work function metal electrodes of UV photo-detector. It shows that as the work function increases, the generating electrons needs more energy to cross the barrier between metal and semiconductor and thus the dark current will reduces.

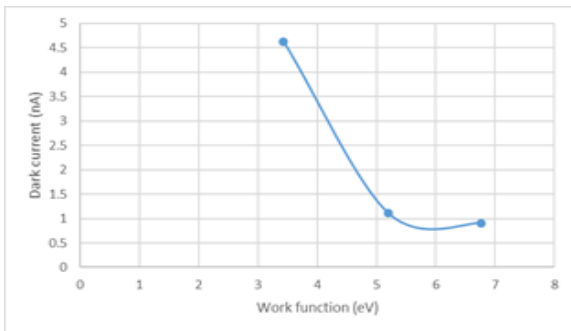


Fig. 16: Dark current response variation with different work function metal electrodes

Figure 16 shows the plot of dark current response with metal electrodes having work functions 3.43 eV, 5.2 eV, 6.76 eV. The MSM structure with non-parallel Schottky barriers have less dark current flow into the device. On analysis, we found the dark currents of the devices are less than 6 nA at 5V. On the other side, the photocurrent of the TiO₂ based photo-detector device have larger value as 297.8 μ A compared to other detectors. On increasing the bias voltage, it is found that the photocurrents gets saturated. This could be overcome by use of Pt electrode having high Schottky barrier. During the application on high biasing, the barrier height will be controlled by applied electric field, tunnelling effect and image force.

B. Variation of dark current with length of active region

Table 3: Variation of dark current with length of TAT thin layer active region.

Length (um)	Dark current (A)
0.055	4.0544×10^{-12}
0.1	7.4205×10^{-12}
0.9	8.1596×10^{-12}
2	5.0266×10^{-11}
10	6.8243×10^{-11}
60	9.5192×10^{-11}
168	8.1139×10^{-10}
362	9.0724×10^{-10}

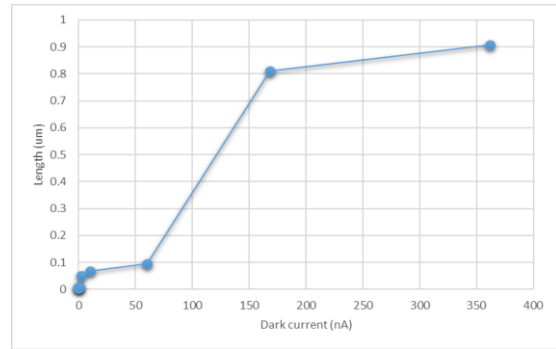


Fig. 17: Dark current response variation with different work function metal electrodes

Figure 17 shows the dark current response variation with length of TAT thin layer active region. It exhibits the variation of length of active region had an obvious effect on photo-electronic properties. When the thickness is from 55 nm – 900 nm, the detector exhibits much lower dark current in the range of nano amperes (nA) and as the length of active region increases, the leakage current also increases due to the availability of larger area for the thermal generation of carriers.

V. CONCLUSION

The 2D photo-detector with 110 nm TiO₂ layer and 3D photo-detector with TAT layer of 362 nm, is designed and simulated using COMSOL 4.4 Multiphysics. The simulation results shows the variation in output current responses with wavelength of incident illumination (ranging from 90 nm to 980 nm). With a 5V applied bias, a maximum photo-response of 0.077 A/W is obtained for conventional 2D structure with TiO₂ layer and 4.9 A/W for proposed TAT layered UV photo-detector. The variation in dark current response for different work function metal electrodes for UV photo-detector and the dependence of dark current characteristics on the thickness of TAT layer thin films are also simulated and investigated using MATLAB. It shows that, as the work function increases, the generating electrons needs more energy to cross the barrier between metal and semiconductor and thus reduction in dark current is obtained.

ACKNOWLEDGMENT

I would like to express my deepest appreciation to all those who provided me the possibility to complete this project. A special gratitude I give to the Department of Electronics and Communication Engineering, Karunya Institute of Technology and Sciences for the support to complete this work. Also, I thank Purdue University to carry out the simulation results.

REFERENCES

1. D. I. Moon, E. Lee, J. H. Yang, K. S. Lim, and Y. K. Choi, "Transparent Zinc Oxide Gate Metal-Oxide-Semiconductor Field-Effect Transistor for High Responsivity Photo-detector," IEEE Electron Device Lett., vol. 30, no. 11, pp. 493-495, May 2009
2. B. S. Choi, S. H. Jo, M. Bae, P. Choi, J. K. Shin, and J. Kim, "CMOS binary image sensor using Gate/Body – tied MOSFET type photo-detector," IEEE Sensors and Materials., vol. 19, no. 7, pp. 1–2, Nov. 2014
3. G. Wang , H. Lu, D. Chen, F. Ren, R. Zhang, and Y. Zheng, "High Quantum Efficiency GaN-Based p-i-n Ultraviolet Photo-detectors Prepared on Patterned Sapphire Substrates," IEEE Photonics Technology Lett., vol. 25, no. 7, pp. 735-738, Apr. 2013
4. H. Wang, P. Parkinson, J. Tian, D. Saxena, S. Mokkaapati, Q. Gao, P. Prasai, L. Fu, F. Karouta, H. H. Tan, and C. Jagadish, "Optoelectronic properties of GaAs nanowire photo-detector," IEEE Device Conf., pp. 139-140, Dec. 2012
5. L. Shi, S. Nihtianov, "Comparitive Study of Silicon-Based Ultraviolet Photo-detectors," IEEE Sensors J., vol. 12, no. 7, pp. 2453-2459, Jul. 2012
6. W. S. Shih, S. J. Young, L. W. Ji, W. Water, T. H. Meen, and H. W. Shiu, "Effect of oxygen plasma treatment on characteristics of TiO2 photo-detectors," IEEE Sensors J., vol. 11, no. 11, pp. 3031–3035, Nov. 2011
7. S. Mohammad Nejad, S. G. Samani, and E. Rahimi, "Characterization of responsivity and quantum efficiency of TiO2 based photo-detectors doped with Ag Nanoparticles," IEEE Photonics Technology Lett., vol. 2, no. 6, pp. 394-397, 2013
8. H. Huang, W. Yang, Y. Xie, X. Chen, and Z. Wu, "MSM Ultraviolet photo-detectors based on TiO2 films deposited by RF Magnetron sputtering," IEEE Electron Device Lett., vol. 31, no. 6, pp. 588-590, Jun. 2010
9. H. Fei Qi, D. Liu, and F. Sun, "The fabrication and characterization of TiO2 UV detector," Journal of crystal Growth, pp. 1-4, Dec. 2012
10. B. Boratynski, B. Paszkiewicz, and M. Szreter "GaN MSM UV photo-detectors," Appl. Phys.Lett., pp. 735-738, Jul. 2003
11. H. Y. Liu, Y. H. Wang, L. and W. C. Hsu, "Suppression of dark current on AlGaIn/GaN MSM photo-detectors," IEEE Sensors J., vol. 11, no. 11, pp. 1–6, May 2015
12. H. Inokawa , H. Satoh, D. Chen, A. Ono, and W. Du, "Evolution of photo-detectors by silicon-on-insulator material," IEEE Trans. Electron Devices., vol. 60, no. 2, pp. 9-13, Apr. 2013
13. A. A. Hussain, A. R. Pal, and D. S. Patil, "High photosensitivity with enhanced photoelectrical contribution in hybrid nanocomposite flexible UV photodetector," Organic Electronics Lett., vol. 15, pp. 2107-2115, Feb. 2014
14. H. T. She, and C. Shu, "Optoelectronic logic devices implemented on GaAs photodetector," IEEE Photon Technol., pp. 54-57, Dec. 1994
15. Y. M. Juan, S. J. Chang, H. T. Hsueh, T. C. Chen, S.W. Huang, Y. H. Lee, T.J. Hsueh "Self – Powered humidity sensor and dual-band UV photodetector fabricated on back-contact photovoltaic cell," Appl. Phys. Lett., pp. 43-49, Dec. 2014
16. S.Sahni, Xi Luo, Jian Liu, Y.H.Xie, Eli Yablonovitch, "JFET based germanium photodetector on silicon-on-insulator," Phys. Rev. B, pp. 3427–3438, Sep. 2008
17. J.L.Huo , S.J. Chang, C.H.Wu, T.J.Hsueh, "Self-Powered ZnO nanowire UV photodetector integrated with GaInP/GaAs/Ge Solar cell," pp. 2661041–2661044, Dec. 2013
18. R.W. Going, Jodi Loo, T.J King Liu, M.C.Wu, "Germanium Gate photoMOSFET integrated on silicon photonics," Mar. 2014
19. D.Yang , Li Zhang, H.Wang , Yishan Wang, Z.Li, T.Song, C.Fu, S.Yang, B.Zou, "Pentacene-based photodetector in visible region with vertical FET configuration," , vol. 80, no. 1, pp. 47–71, 2015
20. H. Xue, "TiO2 based metal-semiconductor-metal UV PDs," Appl. Phys. Lett., vol. 90, no. 20, pp. 2011181–2011183, May. 2007

AUTHORS PROFILE



Alfred Kirubaraj Currently working at Karunya Institute of Technology and Sciences. He presented many papers in International Conferences. Also published several research articles in Scopus index Journal.



Second Author Completed Ph.D. from bharathiar University .Published several books and research papers in reputed Journals. Membership in European Center in Research and Development.



Third Author Completed his PhD from Karunya University and currently pursuing Post-Doctoral Fellowship from Purdue University. Published Many Books and Research Papers in reputed Journals.